

## HOLOGRAPHIC CONDUCTIVITY\*

DAVID TONG

Department of Applied Mathematics and Theoretical Physics  
University of Cambridge  
Wilberforce Road, Cambridge CB3 0WA, United Kingdom

(Received October 16, 2013)

We explain how to compute the conductivity of strongly interacting quantum field theories which have a dual holographic description in terms of gravitational physics in anti-de Sitter space-time.

DOI:10.5506/APhysPolB.44.2579

PACS numbers: 11.25.-w, 72.10.-d

## 1. Introduction

We are going to talk about Ohm's law. We are going to take a strongly interacting quantum field theory, heat it up, throw in a bunch of charged matter and place a (figurative) rusty crocodile clip on either end. Our goal is simply to understand how to calculate the current that passes through this material when we drop a voltage across it.

Rather than attempt this calculation within the framework of quantum field theory, we are going to take a somewhat different approach. There are classes of quantum field theories which have a dual description in terms of gravitational theories in higher dimensions. This duality goes by the name of the *AdS/CFT correspondence* or, sometimes, simply *holography*. The purpose of these lectures is to explain how one can use general relativity and the ideas of holography to extract the physics of conductivity.

This mini-course consists of three lectures. In the first lecture we describe the basics of holography. Although the subject is grounded in string theory, we take a more applied approach, simply focussing on how one can extract correlation functions from classical gravitational theories. In the second

---

\* Lectures presented at the LIH Cracow School of Theoretical Physics "Conformal Symmetry and Perspectives in Quantum and Mathematical Gravity", Zakopane, Poland, June 28–July 7, 2013.

lecture, we describe a few (very) basic facts about conductivity. In the final lecture, we then draw these threads together and explain how to compute the conductivity of strongly interacting theories with holographic duals.

## 2. Basics of holography

The purpose of this first lecture is to provide an introduction to the AdS/CFT correspondence. There are a number of excellent, longer review articles available. The first review article [1] focusses on the connections to string theory and specific supersymmetric gauge theories; more recent reviews [2, 3] have an emphasis on phenomenological applications, typically in the context of condensed matter physics.

Holography is the statement of an equivalence between two very different looking theories:

- Strongly interacting quantum field theories in  $d$  space-time dimensions;
- Theories of gravity in (at least)  $d + 1$  space-time dimensions.

There is a cartoon that illustrates the AdS/CFT correspondence that will be useful to keep in the back of our minds throughout these lectures. It is shown below. The black/blue plane, to the right of this picture, represents the Minkowski space,  $\mathbf{R}^{d-1,1}$  and is usually called the *boundary* of the space. This is where the quantum field theory lives. Properties of this theory will be clarified as we go on, but for now it will suffice to think of it as describing some strongly interacting matter. Here, matter means quantum fields with spin 0, 1/2 or 1. The boundary quantum field theory does not include gravity.

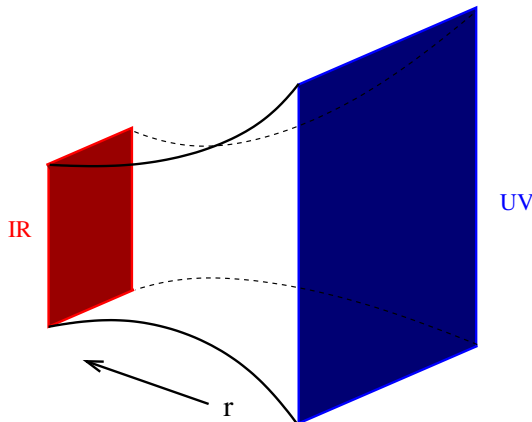


Fig. 1. A cartoon of AdS space.

Stretching away from the boundary is another dimension, labelled with coordinate  $r$  in the diagram. This larger space is usually referred to as the *bulk*. Living inside the bulk is a different theory — a theory of gravity. In practice, this usually means general relativity coupled to a bunch of other fields.

The claim of holography is that these two theories — gravity in the bulk and QFT on the boundary — are equivalent. Anything that happens in the bulk is mirrored in some fashion on the boundary and *vice versa*.

The extra radial dimension,  $r$ , has a very natural interpretation. We learned through the work of Kadanoff and Wilson and others that quantum field theories are organised by length scale, or equivalently by energy scale. The bulk radial direction  $r$  should be interpreted as this length scale. Processes which happen at different slices in the bulk geometry correspond to processes occurring at different wavelengths and energies in the boundary theory. The  $r \rightarrow 0$  part of the bulk geometry corresponds to the ultra-violet (UV) of the field theory, conveniently colour-coded black/blue in the diagram. Meanwhile,  $r \rightarrow \infty$  corresponds to the infrared (IR). In this manner, the AdS/CFT correspondence provides a geometrization of the Wilsonian renormalization group, captured by general relativity in one higher dimension. This statement can be succinctly expressed by the geek joke:  $[G, R] = 0$ .

The first example of the correspondence mapped relativistic conformal field theories (CFTs) on the boundary to gravity in anti-de Sitter (AdS) space in the bulk [4]. This is where the name AdS/CFT derives from. However, it did not take long before examples were found which moved beyond this. For example, we now know of quantum field theories with a mass gap which are dual to curved geometries which are not AdS. We also know of non-relativistic theories which are dual to different geometries which are not AdS. The name “AdS/CFT correspondence” is, therefore, rather limiting: there are many extensions to not-AdS/not-CFT correspondences.

### 2.1. The GKPW formula

For these lectures, we are going to start with the simplest example where the bulk geometry is AdS. We will work in the “Poincaré patch”. This is a slice of global AdS in which the boundary is flat. The metric of the bulk space is

$$ds^2 = \frac{L^2}{r^2} (dr^2 + \eta_{\mu\nu} dx^\mu dx^\nu) . \quad (1)$$

Here,  $L$  is referred to as the AdS scale. The  $\mu, \nu = 0, \dots, d-1$  indices run over the boundary space-time coordinates. The fact that the bulk space-time is AdS means that the boundary theory is conformal. This shows

up, for example, in the symmetry groups. AdS space-time has an  $SO(2, d)$  isometry group. This is the same as the conformal group of the  $d$ -dimensional boundary theory. However, deformations of the geometry away from AdS can be thought of as deformations of the field theory away from the conformal fixed point.

Usually in a quantum field theory, we want to compute the generating function which is schematically of the form

$$Z_{\text{QFT}}[\phi_0] = \int DA \exp \left( i \left[ S_{\text{QFT}} + \int \phi_0 \mathcal{O}(A) \right] \right). \quad (2)$$

Here,  $A$  is shorthand for all the fundamental fields in the theory. These are the things we need to integrate over in the path integral.  $S_{\text{QFT}}$  is the action of the theory; it is a functional of the fields  $A$ . Finally,  $\mathcal{O}(A)$  is an operator of the theory built from the fields  $A$ . It may simply be one of the fundamental fields themselves or it may be some composite operator. The one thing that we will insist upon is that it is gauge invariant.

In the generating function above, the operator  $\mathcal{O}(A)$  is sourced by  $\phi_0(x)$ . This is not dynamical. Rather, it is a fixed function that is under our control. In the context of high-energy physics, we often think about  $\phi_0$  as a mere mathematical trick; differentiating with respect to  $\phi_0$  some number of times and subsequently setting  $\phi_0 = 0$  computes correlation functions of the operator  $\mathcal{O}$ . However, in the context of condensed matter physics, the source  $\phi_0$  is usually something more real. It might be a background electric or magnetic field, or a background pressure density, or a term that arises because some guy is sticking a spoon into your quantum liquid and stirring. In either context, the goal is the same: compute  $Z_{\text{QFT}}[\phi_0]$  for all values of the source  $\phi_0(x)$ .

The basic idea of holography is to breathe life into this source  $\phi_0$ . We promote it from a fixed function to a fully fledged dynamical field that will be governed by its own equations of motion. The trick is that the dynamics for  $\phi_0$  takes place in the higher dimensional bulk, rather than on the boundary. So we have some field  $\phi(x, r)$  that is part of the bulk gravitational theory. We keep a modicum of control over this field only by insisting on its boundary value. Roughly speaking, we will require that  $\phi(x, r) \rightarrow \phi_0(x)$  as we approach the boundary,  $r \rightarrow 0$ . (Although we will have to revisit this naive formula shortly.)

The fundamental formula of holography is the so-called GKPW formula (named after its discoverers Gubser, Klebanov and Polyakov [5] and Witten [6]). It relates the boundary generating function to the bulk partition function

$$Z_{\text{QFT}}[\phi_0] = Z_{\text{QG}} [\text{“}\phi \rightarrow \phi_0\text{” on the boundary}]. \quad (3)$$

Here, “QG” stands for “quantum gravity”: the right-hand side should be thought of as a partition function of quantum gravity in the bulk of AdS. At first sight, that does not seem particularly helpful. It may be hard to compute the generating function of a strongly interacting field theory, but it is surely no more difficult than figuring out quantum gravity. However, there is a limit in which the right-hand side becomes eminently solvable: this is when gravity is classical. Then we can approximate the bulk partition function by its saddle-point to write

$$Z_{\text{QFT}}[\phi_0] \approx e^{iS_{\text{bulk}}|_{\phi \rightarrow \phi_0}} . \quad (4)$$

Now, the right-hand side is simply the on-shell bulk action, subject to the requirement that  $\phi \rightarrow \phi_0$  on the boundary. (Here “on-shell” means that you solve the equations of motion subject to this boundary condition and then plug the answer back into the action.)

This is a lovely and powerful formula. But there is a catch: given a quantum field theory  $S_{\text{QFT}}$ , how do you figure out which bulk theory  $S_{\text{bulk}}$  it corresponds to? And what guarantees that the bulk gravitational theory will be classical to allow you to proceed from the useless (3) to the useful (4)?

This is the tricky part of AdS/CFT. There is certainly no prescriptive way to start from  $S_{\text{QFT}}$  and figure out what the dual gravity theory should be. Instead, finding dual pairs of boundary and bulk theories typically requires input from string theory. There now exist many examples of such pairs, where both  $S_{\text{QFT}}$  and  $S_{\text{bulk}}$  have been identified. The most famous example is  $\mathcal{N} = 4$  super Yang–Mills in  $d = 3 + 1$  dimensions which is dual to type IIB string theory compactified on  $\text{AdS}_5 \times \mathbf{S}^5$ . For all examples, if we want the bulk theory to be well approximated by classical gravity then one requirement is that the boundary theory has a large  $N$  number of degrees of freedom. (For example,  $\text{SU}(N)$  gauge theory in the ’t Hooft limit  $N \rightarrow \infty$ .)

In these lectures, we will take a somewhat different attitude: we will start from a bulk theory of gravity and use this to define a corresponding boundary field theory. Equation (4) provides a map which allows us to compute any correlation function that we desire in the boundary theory. Moreover, we will not be using anything complicated in the bulk: merely Einstein–Maxwell theory. Since this is a component of all known holographic theories (possibly accompanied by a dilaton coupling), you can think of the results below as applying broadly to a wide class of holographic theories.

## 2.2. The dictionary

Above, we have seen that sources in the boundary theory become fields in the bulk. In general, there is a field in the bulk for every operator that you can write down in the boundary theory. That is a lot of fields. (It is related

to the fact that, at least in known examples, the bulk is a string theory with a tower of high-mass states.) However, typically we are only interested in a few boundary operators and, correspondingly, a few bulk fields.

The simplest example maps the source for a scalar operator  $\mathcal{O}(x)$  in the boundary to a scalar field  $\phi(x, r)$  in the bulk

$$\phi(x, r) \longleftrightarrow \mathcal{O}(x).$$

We will explore this in more detail below, where we will see that the mass of the bulk scalar maps into the dimension of the boundary operator.

We could also think about fields of more general spin. Here, there are no surprises: fermionic fields in the bulk map into fermionic operators in the boundary; vector fields in the bulk map into vector operators in the boundary. The most important such example is a bulk gauge field  $A_A(x, r)$ . This maps into a conserved current  $J_\mu$  in the boundary

$$A_A(x, r) \longleftrightarrow J_\mu(x).$$

It is not hard to show that gauge symmetry in the bulk implies conservation of the boundary current:  $\partial^\mu J_\mu = 0$ . (Note that the  $A$  vector index in the bulk runs over one more value than the boundary  $\mu$  index. This does not cause a problem with the dictionary because you can always use gauge invariance to set  $A_r = 0$ .)

Our final example is perhaps the most important. Any theory of gravity necessarily has a bulk metric  $g_{AB}$ . In any holographic theory, this is dual to the energy-momentum tensor in the boundary

$$g_{AB}(x, r) \longleftrightarrow T_{\mu\nu}(x).$$

Here, diffeomorphism invariance in the bulk ensures conservation of the energy and momentum currents:  $\partial^\mu T_{\mu\nu} = 0$ .

### 2.3. An example: the scalar field

Many of the most basic features of the map between bulk and boundary can be illustrated with a toy model. (More details of this toy model, together with models that are less toy, can be found in [7].) For these purposes, we will forget about gravity completely for now and just work with a free scalar field in a fixed background  $d + 1$ -dimensional AdS space. The action is

$$S_{\text{scalar}} = -\frac{1}{2} \int d^{d+1}x \sqrt{g} [g^{AB} \partial_A \phi \partial_B \phi + m^2 \phi], \quad (5)$$

where  $g^{AB}$  is the (inverse) AdS metric (1). The equation of motion for the scalar is

$$\partial_A (\sqrt{-g} g^{AB} \partial_B \phi) - \sqrt{-g} m^2 \phi = 0. \quad (6)$$

Since we have translational invariance in the direction parallel to the boundary, we can always Fourier transform and work with the ansatz  $\phi = \phi(r)e^{ik \cdot x}$ . The equation of motion becomes

$$-r^{d+1}\partial_r \left( r^{-d+1}\partial_r\phi \right) + (k^2r^2 + m^2L^2)\phi = 0, \tag{7}$$

where  $k^2 = -\omega^2 + \vec{k}^2$ , with  $\omega$  is the frequency and  $\vec{k}$  the spatial momentum.

The solution to this equation is given by a Bessel function. But, for our immediate purposes, we will only need the behaviour of the solution as we approach the boundary at  $r = 0$ . For this, we can drop the  $k^2$  term, and try the ansatz

$$\phi \sim r^\Delta. \tag{8}$$

This solves the equation above if  $\Delta(\Delta - d) = m^2L^2$ , which has roots

$$\Delta_\pm = \frac{d}{2} \pm \sqrt{\frac{d^2}{4} + m^2L^2}. \tag{9}$$

We learn that the general near-boundary behaviour of a scalar field in AdS is

$$\phi(r) \rightarrow \left(\frac{r}{L}\right)^{\Delta_-} [\phi_0(x) + \dots] + \left(\frac{r}{L}\right)^{\Delta_+} [\phi_1(x) + \dots]. \tag{10}$$

Let me make a few comments about this simple, but important, result.

Earlier, I said that we should fix  $\phi \rightarrow \phi_0$  on the boundary of AdS. But the calculation above shows that this cannot be right! (In fairness, I did place this equation in quotation marks in (3) and (4); this was supposed to be a hint that it needed amending!) If we want to solve the equations of motion, we should really impose the boundary conditions

$$\phi \rightarrow \left(\frac{r}{L}\right)^{\Delta_-} \phi_0(x) \tag{11}$$

as the  $\phi$  approaches the boundary. We will interpret the function  $\phi_0(x)$  as the source in the boundary field theory.

Note that both roots  $\Delta_\pm$  are real whenever

$$m^2 \geq -\left(\frac{d}{2L}\right)^2. \tag{12}$$

That is rather surprising. It means that, at least within the calculations above, nothing bad happens for masses above this bound. In particular, the mass-squared can be a little bit negative and that is OK. This is known as the Breitenlohner–Freedman (or BF) bound: scalar fields can be a little bit tachyonic in AdS and still be stable.

### 2.4. Linear response

Let us ask a question. We have identified  $\phi_0(x)$  in (10) as the source in the field theory. What is the interpretation of the other independent function in the solution,  $\phi_1(x)$ ?

The answer to this question is the key to many holographic calculations. It is

$$\phi_1(x) = \langle \mathcal{O}(x) \rangle. \quad (13)$$

The value of  $\phi_1(x)$  measures the one-point function of the operator  $\mathcal{O}$  in the presence of the source  $\phi_0$ . In other words,  $\phi_1$  is telling you the response of the operator to the source.

I will now sketch why equation (13) is true. We can always compute the one-point function in a quantum field theory by differentiating the generating function

$$\langle \mathcal{O} \rangle = \frac{1}{Z_{\text{QFT}}} \frac{\partial Z_{\text{QFT}}[\phi_0]}{\partial \phi_0} = \frac{\partial \log Z_{\text{QFT}}[\phi_0]}{\partial \phi_0} = \frac{\partial S_{\text{bulk}}[\phi_0]}{\partial \phi_0}, \quad (14)$$

where, in the final equality, we have used (4). Recall that  $S_{\text{bulk}}[\phi_0]$  is the on-shell bulk action, subject to fixed boundary conditions (11). We want to know what happens to this on-shell action as we vary the boundary conditions.

This kind of question is reminiscent of Hamilton–Jacobi theory in classical mechanics. Let us briefly remind ourselves how Hamilton–Jacobi theory works in the simplest case of a point particle. When you vary the action for a point particle with position  $q$ , you get two kinds of terms

$$\delta S_{\text{particle}} = \int_{t_i}^{t_f} dt \left[ \frac{\partial L}{\partial q} - \frac{d}{dt} \left( \frac{\partial L}{\partial \dot{q}} \right) \right] \delta q + \left[ \frac{\partial L}{\partial \dot{q}} \delta q \right]_{t_i}^{t_f}. \quad (15)$$

When deriving the equations of motion, we fix the boundary conditions so that  $\delta q(t_i) = \delta q(t_f) = 0$  and the second term vanishes. Insisting that  $\delta S = 0$  then gives us the equations of motion which sit inside the first term above.

But in Hamilton–Jacobi theory, we turn this on its head. We are interested in the *on-shell* action, which means that we evaluate the action on the equations of motion. The on-shell action is a function only of the boundary value of fields,  $q_i = q(t_i)$  and  $q_f = q(t_f)$ . Suppose that we change the final position of the particle. Equation (15) still tells us how the on-shell action changes, but now the first term vanishes because the fields are on-shell. We are left instead with

$$\frac{\partial S[q_i; q_f]}{\partial q_f} = \left. \frac{\partial L}{\partial \dot{q}} \right|_{t_f} = p_f. \quad (16)$$

This tells us that varying the on-shell action with respect to the final position gives us the final momentum of the particle.

We can apply the analog of the Hamilton–Jacobi equation (16) to our scalar field in AdS. A little thought will convince you that the correct generalisation is

$$\frac{\partial S}{\partial \phi_0} = \left(\frac{r}{L}\right)^{\Delta-} \frac{\partial \mathcal{L}}{\partial(\partial_r \phi)} \Big|_{r=0}, \quad (17)$$

where the extra power of  $(r/L)^{\Delta-}$  arises because the boundary condition is given by (11). Now we are almost done. It just remains to compute  $\partial \mathcal{L} / \partial \phi'$ . I will leave this as an exercise. Completing the proof shows that

$$\langle \mathcal{O} \rangle \sim \phi_1 \quad (18)$$

as promised. (There is, in fact, a subtlety in this calculation which I am brushing under the carpet. Boundary terms are necessary in the bulk action, both to have a well defined variational principle and to avoid divergences in the on-shell action. A correct treatment of these boundary terms is necessary to get the coefficient right in (18).)

Nearly all applications of holography boil down to implementing some version of the response calculation sketched above. There is a general strategy that one takes in all these holographic calculations, which is as follows:

- Fix  $\phi_0$  as  $r \rightarrow 0$ .
- Since the equations of motion for  $\phi$  are second order, we need another boundary condition. This is imposed in the infrared of the geometry (*i.e.* as  $r \rightarrow \infty$ ). Exactly what boundary condition we impose depends on the context. If we are working in Euclidean signature, we typically require that fields do not diverge in the interior of the geometry. If we are working in Lorentzian signature, we typically require some kind of ingoing boundary condition in the interior. (We will see examples in Section 4.)
- With these two boundary conditions in place, we now solve the equations of motion and extract the response of the system  $\phi_1$ .

The main purpose of these lectures is to perform these calculations in situations where the source is a background electric field and the response is a current. This allows us to compute the conductivity of our theory. Before we delve into this, we take a small diversion to review some basic features that we expect from conductivity in different systems.

### 3. Basics of conductivity

In this section, we leave ideas of holography behind. Instead, we will take something of a diversion to explain a few basic features of conductivity. Our goal is to simply review some essential facts in order to place the holographic calculations of the next section in some kind of context.

We all learned about Ohm's law in kindergarten. It is " $V = IR$ ", relating the voltage drop  $V$  to an induced current  $I$ . The ratio is the resistance  $R$ . Here we work in slightly more grown-up language. We will discuss the induced current density  $\vec{j}(t, \vec{x})$  due an applied electric field  $\vec{E}(t, \vec{x})$ .

In what follows, we will work with an electric field that is constant in space, but varying in time. It is most convenient to work with the Fourier transform of the fields vibrating at some fixed frequency  $\omega$

$$\vec{E}(t) = \int \frac{d\omega}{2\pi} e^{-i\omega t} \vec{E}(\omega), \quad \vec{j}(t) = \int \frac{d\omega}{2\pi} e^{-i\omega t} \vec{j}(\omega). \quad (19)$$

In this notation, Ohm's law reads

$$\vec{j}(\omega) = \sigma(\omega) \vec{E}(\omega). \quad (20)$$

Note that if we shake the electric field at frequency  $\omega$ , then the system responds at the same frequency  $\omega$ . This is the regime of linear response.

The ratio  $\sigma(\omega)$  is the *optical conductivity*. Since we are working in Fourier space,  $\sigma$  is complex. The real part captures what you would intuitively call the conductivity (or inverse resistivity) of the system: it describes the dissipation of the current. The imaginary part is the reactive part. We will illustrate this with some examples below.

#### 3.1. The Drude model

Let us go right back to basics. The Drude model is a simple description of charge transport, based on the idea of billiard ball-like charge carriers bouncing off things in a solid. It is nothing more than Newtonian physics. However, rather surprisingly, several features of the Drude model are extremely robust, surviving many subsequent revolutions in physics. Indeed, in the next section, we will see aspects of the Drude model emerging from general relativity! But we are getting ahead of ourselves ...

Consider a particle of mass  $m$ , charge  $q$  and velocity  $\vec{v}$ . The essence of the Drude model is Newtonian " $F = ma$ ", where the force is due to the electric field, together with a linear friction term

$$m \frac{d\vec{v}}{dt} + \frac{m}{\tau} \vec{v} = q\vec{E}. \quad (21)$$

The coefficient  $\tau$  is known as the *scattering time*. It can be thought of as the average time that the particle travels unimpeded before it hits something.

The current is  $\vec{j} = nq\vec{v}$ , where  $n$  is the density of charge carriers. For an AC electric field, with frequency  $\omega$ , we need only solve (21) to determine the steady-state current  $\vec{j}(\omega)$ . The definition (20) then tells us the conductivity: it is

$$\sigma(\omega) = \frac{\sigma_0}{1 - i\omega\tau}, \tag{22}$$

where the  $\omega \rightarrow 0$  DC conductivity is

$$\sigma_0 = \frac{nq^2\tau}{m}.$$

We plot the real and imaginary parts of the conductivity in figure 2. The real part exhibits a peak at frequencies  $\omega < 1/\tau$ ; this will be referred to below as the Drude peak. At high frequencies,  $\omega\tau \gg 1$ , the conductivity is dominated by the imaginary part,  $\sigma \sim -1/i\omega$ . This is the conductivity of a free particle. You can think about this as shaking the particle so fast that it turns around and goes the other way before it had the chance to hit something.

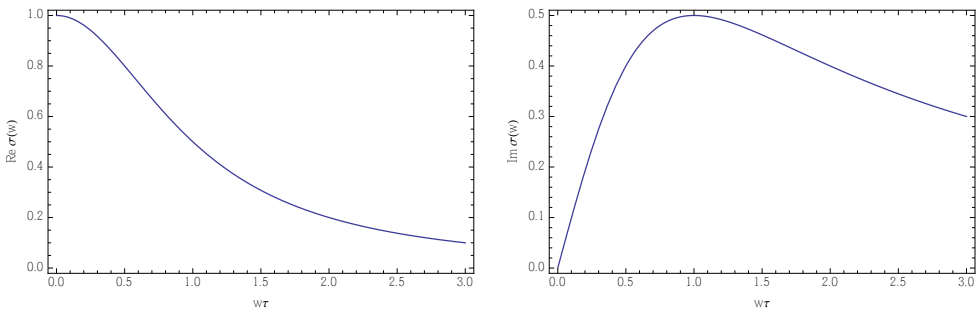


Fig. 2. The real and imaginary parts of the Drude conductivity.

### 3.2. Particle-hole creation

At high frequencies, there is another simple effect that can contribute to conductivity. This is not captured by the Drude model, but is instead a quantum field-theoretic effect, namely particle-anti-particle creation. Or, in a condensed matter context, particle-hole creation. It is perhaps simplest to illustrate by showing some data.

Figure 3 shows the real part of the conductivity of graphene, taken from [8]. For our purposes, graphene should be thought of as relativistic quantum field theory in the lab. It is a particularly simple relativistic quantum field theory in  $d = 2 + 1$  dimensions, consisting of four, free Dirac fermions. The plots shown in the figure are not measured at the relativistic Dirac point, but instead at finite chemical potential. The curves that lie further to the right correspond to systems with higher Fermi energy  $E_F$ .

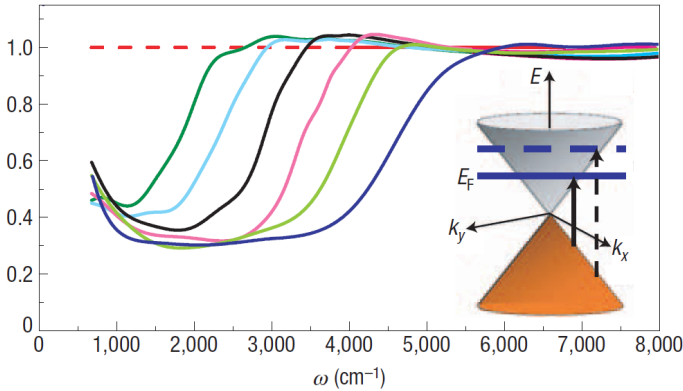


Fig. 3. The optical conductivity of graphene, taken from [8].

At low frequencies, we can see the beginning of the Drude peak. But at higher frequencies, the conductivity begins to rise again, signalling the presence of new charge carriers, before levelling off. The rise happens around  $\omega \sim 2E_F$ . At these frequencies, we can excite electrons from the filled valence band into the conduction band, and these particle-hole pairs then contribute to the charge density. (Note that the excited electron must have the same momentum as the hole, which is why the  $2E_F$  energy is required.)

There is also interesting physics contained in the plateau region at very high energy. The fact that the conductivity does not change is telling us that we have a scale invariant theory: we get the same physics at all scales. This statement is specific to theories in  $d = 2 + 1$  dimensions. To see this, we can do some naive dimension counting: the dimension of the electric field is always  $[E] = 2$ . The dimension of a conserved current density in  $d$  space-time dimensions is always  $[J] = d - 1$ . This means that the dimension of the conductivity is  $[\sigma] = d - 3$ . So in  $d = 2 + 1$  dimensions, the conductivity is dimensionless and in any conformal field theory, it necessarily reaches a constant value. (In  $d = 3 + 1$ , the conformal behaviour of the conductivity is  $\sigma \sim \omega$ .) The height of the plateaux is telling us the number of charged degrees of freedom in the game: roughly speaking, it is the coefficient of the  $\langle JJ \rangle$  correlation function. In the present case, one can determine that

there are indeed four Dirac electrons in graphene from the height of the conductivity plateaux. For more details of conductivity at quantum critical points, see [9].

### 3.3. A strongly interacting material

The charge carriers in graphene are essentially free and their dynamics is well understood. To end this section, we make some brief comments on strongly interacting systems that are not so well understood. There are a large number of such systems in nature, including heavy fermion materials and various classes of unconventional superconductors, of which the cuprates are perhaps the most prominent example. These cuprates are effectively two-dimensional, with charge transport taking place in copper-oxide planes.

At optimal doping, above the transition temperature, the cuprates sit in a phase that is often called the “strange metal”. Here, they exhibit many anomalous transport properties. (See, for example, [10] for a basic but very readable account of these materials.) The system is strongly coupled and various experiments strongly imply that there are no well-defined quasi-particles in the system. There are also suggestions that the physics in this region may be governed by a quantum critical point. In this sense, it is similar to the kind of theories studied using holography. (Although, of course, in detail the underlying physics is nothing at all like the theories studied using holography!)

The most famous of the anomalous transport properties is the DC resistivity,  $\rho = \sigma(\omega = 0)$ , which grows linearly with temperature

$$\rho \sim T.$$

In many materials, this behaviour is seen over a couple of orders of magnitude. Its underlying cause is not understood. (For some grounding, the expected behaviour for resistivity dominated by strong electron interactions is  $\rho \sim T^2$ , arising from umklapp scattering. Electron-phonon interactions give  $\rho \sim T^5$  below the Debye temperature and, encouragingly,  $\rho \sim T$  above the Debye temperature. However, the linear DC resistivity seen in the cuprates extends way below the Debye temperature.)

Anomalous behaviour is also seen in the optical conductivity. At low frequencies — roughly  $\omega < T$  — the material exhibits the kind of the Drude peak we described above. But at higher frequencies, there is a surprise. The conductivity flattens out and now exhibits a power-law behaviour. In the left-hand side of figure 4, we show a log-log plot of the absolute part of the conductivity  $|\sigma(\omega)|$  in BiSCCO, taken from [11]. Over a large range, the conductivity scales as

$$|\sigma| = \frac{B}{\omega^\gamma},$$

where  $\gamma \approx 2/3$ . Moreover, the coefficient  $B$  is independent of temperature. (This can be seen in the plots by the fact that all the lines — each plotted at a different temperature — sit directly on top of each other in the scaling regime.) At the same time, the phase of the conductivity, shown in the figure on the right, is constant, around  $60^\circ$ , compatible with the holomorphic behaviour  $\sigma \sim 1/(i\omega)^{2/3}$ . This scaling behaviour is poorly understood. (See [12–14] for models which attempt to explain it.)

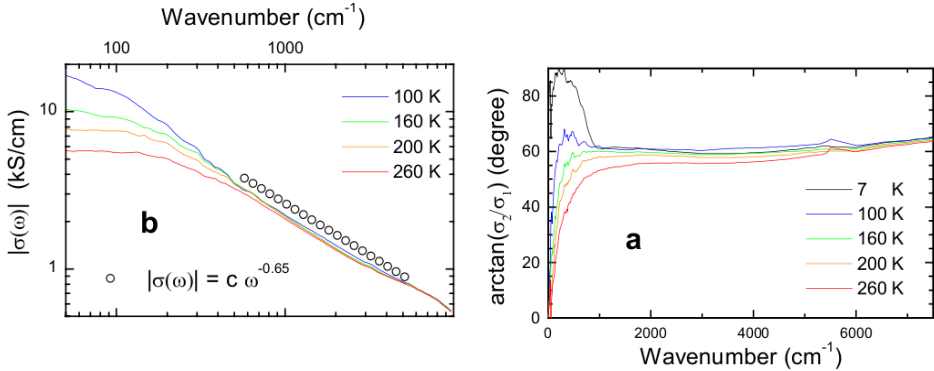


Fig. 4. The optical conductivity of optimally doped  $\text{Bi}_2\text{Sr}_2\text{Ca}_{0.92}\text{Y}_{0.08}\text{Cu}_2\text{O}_{8+\delta}$ , taken from [11].

Note that the cuprates do not exhibit the rise in the conductivity due to particle–hole creation. However, the Fermi energy  $E_F$  is much higher in these systems, nestling at the lattice scale where one no longer expects simple universal behaviour.

With this quick background to the optical conductivity, let us now return to our (much more!) theoretical study of charge transport in strongly coupled holographic models.

#### 4. Holographic conductivity

Let us now get back to the world of holography. For the remainder of these lectures, we are going to work with a  $d = 3 + 1$  dimensional bulk, corresponding to a  $d = 2 + 1$  dimensional boundary theory. We chose Einstein–Maxwell theory

$$S_{\text{bulk}} = \int d^4x \sqrt{-g} \left[ \frac{1}{2\kappa^2} \left( R + \frac{6}{L^2} \right) - \frac{1}{4e^2} F_{AB} F^{AB} \right]. \quad (23)$$

The negative cosmological constant  $\Lambda = -3/\kappa^2 L^2$  is tuned so that the ground state is the AdS metric (1) with curvature scale  $L$ .

As we reviewed in Section 2, the metric is dual to the boundary stress tensor  $T_{\mu\nu}$  and the gauge field is dual to a conserved current  $J_\mu$ . We will not turn on any other fields in the bulk, but all the results that we describe below will hold for any bulk theory with an Einstein–Maxwell sector

We will compute the conductivity associated to the current  $J_\mu$ . Before we do this, there are a few rudimentary concepts that we need to introduce into our gravitational model. These are the temperature and chemical potential of the boundary theory. As we now review, both are associated with black holes in the bulk.

#### 4.1. Black holes

The first thing that we want to do is to place the boundary theory at some finite temperature  $T$ . This is done by placing a black hole in the bulk of AdS [15]. In the Poincaré patch, the black hole is really a black brane; the horizon lies parallel to the (spatial) boundary.

There are a few ways to see that the black hole corresponds to thermal field theory. Perhaps the easiest is to Wick rotate to Euclidean signature. Equilibrium thermal physics in quantum field theories is captured by compactifying Euclidean time with period  $\beta = 1/T$ . Solving the bulk equations of motion with a such a compact Euclidean circle, one finds the Euclidean AdS black hole.

Wick rotating back to Lorentzian signature, we have the AdS Schwarzschild black hole with metric

$$ds^2 = \frac{L^2}{r^2} \left( -f(r)dt^2 + \frac{dr^2}{f(r)} + \eta_{\mu\nu}dx^\mu dx^\nu \right) \quad (24)$$

and

$$f(r) = 1 - \left( \frac{r}{r_h} \right)^3 \quad (25)$$

so that the black hole horizon sits at  $r = r_h$ , where  $f(r) = 0$ . The claim is that this background continues to describe the boundary field theory at finite temperature, now in Lorentzian signature. The temperature of the boundary is given by the Hawking temperature of the black hole

$$T = \frac{3}{4\pi r_h}. \quad (26)$$

However, in Lorentzian signature, the identification of the black hole with a thermal field theory is much more powerful than the corresponding identification in Euclidean space. This is because the bulk no longer captures only

equilibrium physics. Instead, dynamics in the bulk space-time corresponds to real time dynamics in the boundary thermal field theory. Usually, it is rather challenging to do such computations in field theory. But, within the context of holography, it is conceptually trivial: we simply need to solve the time dependent Einstein equations. This ease with which one can compute transport properties — even far from equilibrium transport — is one of the real powers of holography. Note, in particular, that dynamics at finite temperature exhibits a new phenomenon that does not arise at zero temperature: dissipation. This is captured in the bulk by stuff falling into the black hole horizon.

We should elaborate on this a little more. In Section 2.4, we briefly mentioned that, when performing holographic calculations, you must impose some appropriate boundary conditions in the infrared of the geometry. In the presence of the black hole, this means appropriate boundary conditions at the horizon. But which boundary conditions? In fact, we have a choice and this choice corresponds to the choice of Lorentzian propagator in the boundary field theory. The most useful and physically motivated choice is simply to impose ingoing boundary conditions on the horizon, ensuring that stuff only falls into the black hole and nothing comes out. In the boundary field theory, this corresponds to working with retarded propagators. This is the choice relevant for linear response calculations. (Had we imposed outgoing boundary conditions at the horizon, we would have advanced propagators on the boundary.) For more details of this relationship, see [16].

So black holes in the bulk correspond to placing the boundary field theory at some finite temperature. We would now like to throw in a finite density of stuff in the boundary which is achieved by placing the theory at a chemical potential  $\mu$ . This corresponds to charging the black hole, so it emits an electric field [17]. This is the Reissner–Nordström black hole solution. It again has metric (24), now with the function  $f(r)$  taking the form

$$f(r) = 1 - \left(1 + \frac{r_h^2 \mu^2}{\gamma^2}\right) \left(\frac{r}{r_h}\right)^3 + \frac{r_h^2 \mu^2}{\gamma^2} \left(\frac{r}{r_h}\right)^4. \quad (27)$$

The horizon is again at  $r = r_h$ , where  $f(r_h) = 0$ . The coefficient  $\gamma$  is a ratio of the gravitational and electromagnetic couplings

$$\gamma = \frac{2e^2 L^2}{\kappa^2}. \quad (28)$$

The Hawking temperature of the black hole horizon is now given by

$$T = \frac{1}{4\pi r_h} \left(3 - \frac{r_h^2 \mu^2}{\gamma^2}\right). \quad (29)$$

Meanwhile, the temporal component of the gauge field takes the form

$$A_0 = \mu \left( 1 - \frac{r}{r_h} \right). \tag{30}$$

Note that  $A_0 = 0$  at the horizon. This is necessary because the Killing vector  $\partial/\partial t$  degenerates at the horizon and the gauge field  $A_0$  is ill-defined unless it vanishes there.

From our discussion in Section 2, we can read off the physics from the profile of  $A_0$ . We know that in the boundary field theory the gauge field couples to a conserved current,  $\mathcal{L}_{\text{boundary}} \sim A_\mu J^\mu$ . The leading order term in  $A_0$  should be interpreted as the source for  $J^0$ . This is indeed the chemical potential  $\mu$ . Meanwhile, the subleading term should be interpreted as the expectation value  $\langle J^0 \rangle$ , which is simply the charge density. We see that

$$\langle J^0 \rangle \sim \frac{\mu}{r_h}. \tag{31}$$

We can then use (29) to re-express  $r_h$  in terms of  $T$  and  $\mu$ .

#### 4.2. Computing conductivity

The Reissner–Nordström black hole describes the boundary field theory at finite temperature and density. Now, we want to perturb the boundary by turning on an electric field with frequency  $\omega$ . This is a source for the current  $J_x$ . We would like to extract the response of the current  $\langle J_x \rangle$ .

We can implement this using the basic techniques described in Section 2.4. We work with an electric field in the  $A_x$  direction and turn on a source  $A_x = (E/i\omega)e^{i\omega t}$  on the boundary. Obviously, then, the electric field is  $\dot{A}_x = Ee^{i\omega t}$  as required. In the bulk, the leading order terms in  $A_x$  take the form

$$A_x = \frac{E}{i\omega} e^{i\omega t} + \langle J_x \rangle r + \dots \tag{32}$$

As described above, we impose ingoing boundary conditions for  $A_x$  at the horizon of the black hole. Our goal is to determine the sub-leading fall-off  $\langle J_x \rangle$  by solving the equations of motion in the bulk.

These calculations were first performed in [18] for the Schwarzschild black hole and in [2] for the Reissner–Nordström black hole. One can show that sourcing  $A_x$  in this way will also turn on the metric component  $g_{tx}$ , but no further fields. The Maxwell equation is

$$(f(r)A'_x)' + \frac{w^2}{f(r)}A_x = -\frac{A'_0 r^2}{L^2} \left( g'_{tx} + \frac{2}{r}g_{tx} \right),$$

while the Einstein equations require

$$g'_{tx} + \frac{2}{r}g_{tx} + \frac{4L^2}{\gamma^2}A'_0A_x = 0.$$

We can use this latter constraint to eliminate the metric, leaving us with a single second order equation of motion for  $A_x$

$$(fA'_x)' + \frac{w^2}{f}A_x = \frac{4\mu^2}{\gamma^2r_h^2}r^2A_x. \tag{33}$$

Solving this equation, subject to the ingoing boundary conditions at the horizon, allows us to determine the response  $\langle J_x \rangle$  in terms of the source. The ratio is the optical conductivity, which we can write as

$$\sigma(\omega) = \frac{1}{e^2} \frac{A'_x}{i\omega A_x} \Big|_{r=0}. \tag{34}$$

Although (33) cannot be solved analytically, it is a simple matter to solve it numerically. The result is plotted in figure 5.

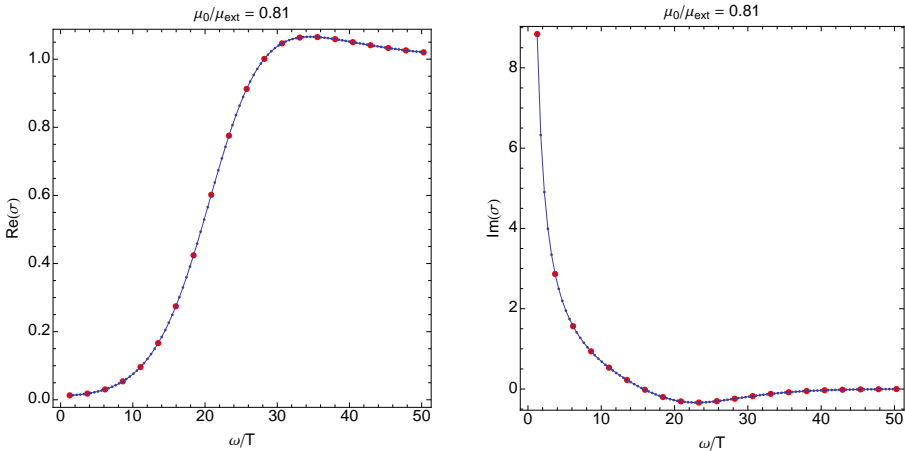


Fig. 5. Holographic optical conductivity.

Let us compare this to our expectations from the previous section. We see that at frequencies  $\omega \geq \mu$ , there is a rise in the conductivity, before it reaches a plateau for higher  $\omega$ . This is analogous to the behaviour seen in graphene and, as we mentioned in Section 3, is typical of any CFT in  $d = 2 + 1$  dimensions.

However, there is no Drude peak at small frequencies. Instead, something much more dramatic happens. In the numerical data shown, this reveals itself as a pole in the imaginary part of the conductivity,  $\text{Im} \sigma \sim 1/\omega$ .

But the Kramers–Kronig relation (which is essentially the requirement of causality imposed on response functions) means that this pole is necessarily accompanied by a zero-frequency delta-function in the real part of the conductivity

$$\text{Re } \sigma(\omega) \sim K\delta(\omega). \quad (35)$$

This delta function does not show up in the numerical plots above. But it is there, lurking. It should be thought of as the Drude peak (22) with the scattering time  $\tau \rightarrow \infty$ .

The existence of this delta-function is not surprising. In fact, it follows from very general considerations. We have a system with a background charge density and with translational invariance. If you subject the system to a constant,  $\omega = 0$ , electric field then the charge density will necessarily accelerate. However, because there is translational invariance, there is momentum conservation. This means that there is no way for the charges to dissipate their momentum and the current will persist. This is the origin of the delta-function (35).

Of course, in real materials, there is no translational invariance. Even in the absence of impurities, there is a background lattice structure which means that, through umklapp processes, momentum is only conserved modulo the lattice momentum. If we want to understand the conductivity in these strongly interacting field theories, we are going to have to introduce the physics of translational symmetry breaking to tease apart that delta-function. In the remainder of these lectures, we will see how to do this.

#### 4.3. A black hole lattice

The most direct way to implement translational symmetry breaking is by introducing a spatially modulated source. For example, we could choose to introduce a chemical potential that varies in space

$$\mathcal{L} = \mathcal{L}_{\text{CFT}} + \mu(x, y)J^0. \quad (36)$$

To do this holographically, we must solve the bulk Einstein–Maxwell equations, subject to the boundary condition  $A_0 \rightarrow \mu(x, y)$  as  $r \rightarrow 0$ . That is not possible analytically. Instead, we need to turn to numerics.

Working with a general function  $\mu(x, y)$  would require solving three-dimensional PDEs with the radial direction providing the third variable. Here we do something a little easier. We work instead with a striped chemical potential of the form

$$\mu = \bar{\mu} (1 + A_0 \cos(kx)). \quad (37)$$

This now requires solving PDEs in two variables. The solutions were found numerically in [19]. They are, as you may expect, rippled Reissner–Nordström black holes. We refer to this as a *holographic lattice*.

With the solutions in hand, it is conceptually straightforward to determine the conductivity using the same method described in the previous section, running the electric field in the  $x$ -direction, against the grain of the stripes. However, while conceptually straightforward, it is computationally challenging. In the case with translational invariance, sourcing  $A_x$  turned on only  $g_{tx}$ . In the absence of translational invariance, almost everything is sourced. One ends up with ten, coupled PDEs in two independent variables, linearised around the numerical rippled Reissner–Nordström black holes. These equations were solved numerically in [19, 20].

The real and imaginary parts of optical conductivity in the presence of a holographic lattice is shown in figure 6. (The black dotted line is the conductivity in the absence of a source that we saw previously in figure 5.) At high frequencies,  $\omega \sim \mu$ , the conductivity is unchanged. The main difference is at low-frequencies where the breaking of translational invariance has resolved the delta-function. (We can see this most clearly in the imaginary part which is now dipping back towards zero at low-frequencies.) We will now look a little more closely at the form of the optical conductivity.

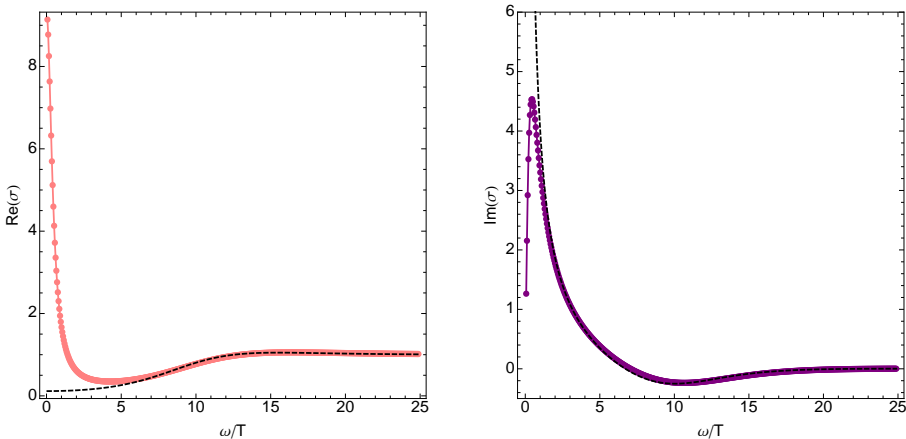


Fig. 6. Holographic optical conductivity in the presence of a lattice, taken from [20].

At the lowest frequencies — roughly  $\omega \leq T$  — the conductivity is very well approximated by the Drude form (22)

$$\sigma(\omega) = \frac{K\tau}{1 - i\omega\tau}. \quad (38)$$

This is shown in figure 7. Here,  $K$  is the coefficient of the delta-function in

the absence of the lattice (35). (This is because there is a sum rule which says that the area under the curve should remain the same.) Meanwhile, the scattering time  $\tau$  is extracted from the numerical data by fitting to this curve. Already here there is, perhaps, something of a surprise. The original Drude formula was derived by thinking about billiard balls moving under Newtonian physics. Here, we have found the same result from general relativity. There are no billiard balls in sight! The Drude form continues to hold in systems that have no quasi-particle description. What is really required is not the existence of quasi-particle, but rather that the time-scale for momentum dissipation remains much longer than any other process.

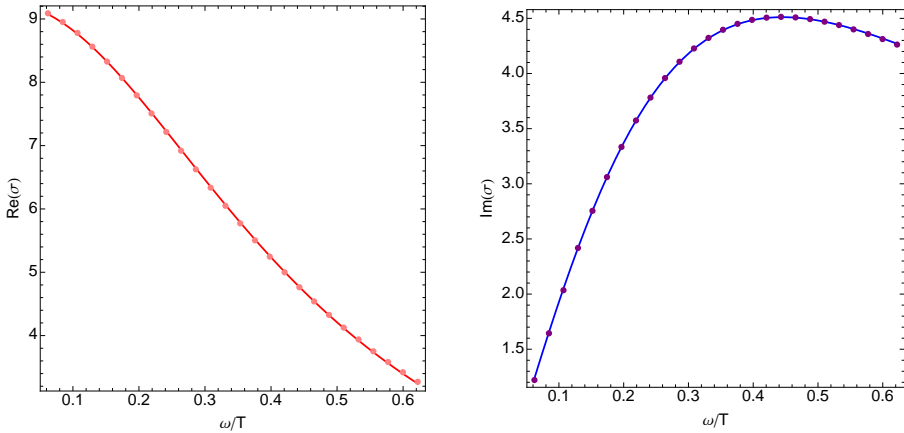


Fig. 7. The low frequency Drude form of the conductivity, taken from [20].

The low-frequency behaviour allows us to extract the scattering time  $\tau(T)$ . It also allows a direct measurement of the DC,  $\omega \rightarrow 0$ , conductivity. In fact, in this limit, one can make analytic progress by thinking about irrelevant perturbations of the infrared geometry of the black hole [21]. (The IR geometry is  $\text{AdS}_2$  and reflects the fact that the boundary theory flows to a so-called *locally critical* fixed point in which time scales, but space does not.) This analysis predicts a form for the resistivity

$$\rho = \frac{1}{K\tau} \sim T^{2\nu-1}, \tag{39}$$

where the exponent  $\nu$  depends on the lattice spacing  $k$  and the chemical potential  $\mu$  in a complicated manner:

$$\nu = \frac{1}{2} \sqrt{5 + 2 \left(\frac{k}{\mu}\right)^2} - 4 \sqrt{1 + \left(\frac{k}{\mu}\right)^2}. \tag{40}$$

This result is confirmed by the numerical work of [20]. Clearly, our holographic models do not give a universal linear resistivity as seen in so many materials. Instead, the resistivity of locally critical theories is more complicated. Nonetheless, a mechanism has been suggested to drive this system to linear resistivity  $\rho \sim T$  [22].

At higher frequencies, the conductivity deviates from the Drude form and flattens out. There is a regime in which the conductivity appears to be well-defined by a powerlaw, albeit with an off-set

$$|\sigma(\omega)| = \frac{B}{\omega^\gamma} + C.$$

To within numerical accuracy, the exponent is given by  $\gamma \approx 2/3$ . This is depicted in the log-log plot in figure 8 in which the conductivity is shown at three different temperature.

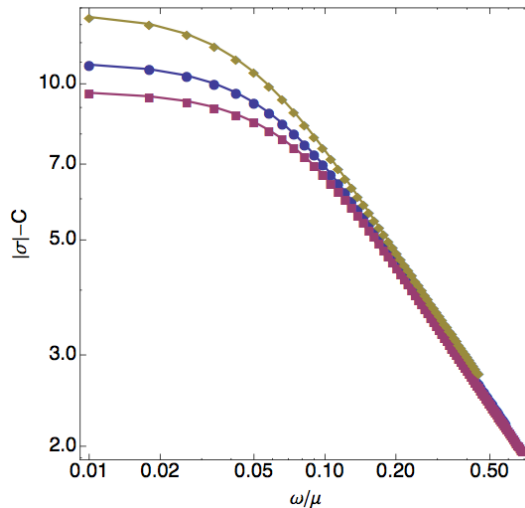


Fig. 8. The intermediate conductivity, taken from [19].

For all value of the parameters, the powerlaw seems to hold in the region  $2 < \omega\tau < 8$ . In the same region, the phase of the conductivity hovers around  $\arg(\sigma) = 65^\circ$  to  $70^\circ$ . Note, however, that the powerlaw is not seen over a parametrically large range of frequencies. Instead, it seems to be emerging from the delta-function, or Drude peak, and both lower and upper-limits are dictated by  $1/\tau$ .

Given that the powerlaw extends over less than an order of magnitude, why should we care? There are two striking features. The first is that the exponent  $\gamma = 2/3$  is robust against changing all parameters: temperature  $T$ , chemical potential  $\mu$ , lattice height  $A_0$  and lattice spacing  $k$ . In contrast, the

other variables  $\tau$ ,  $B$  and  $C$  do change by order one when we vary different parameters. The second feature is that the coefficient  $B$  is independent of temperature. This is seen clearly in figure 8, where the curves sit on top of each other when they reach the powerlaw regime.

Notably, both the exponent and the independence of  $B$  on temperature coincide with the optical conductivity seen in the cuprates that we described in Section 3.3. We do not know if this is coincidence, or if it points towards something deeper. It is worth stressing that the powerlaw in the cuprates extends over several orders of magnitude and does not require a significant off-set  $C$ .

Similar powerlaws are seen in other observables in the same region, including thermoelectric conductivity in  $d = 2 + 1$  and optical conductivity in  $d = 3 + 1$  dimensions [19] (with different exponents). For all of these powerlaws, there is currently only numerical evidence.

#### 4.4. Summary

The purpose of these lectures is to explain how one can use holography to compute the conductivity of certain strongly interacting field theories. As we have seen, the holographic dictionary allows us to extract some familiar condensed matter physics out of these gravitational systems, while providing quantitative information about charge transport in this class of field theories.

My thanks to Gary Horowitz and Jorge Santos for enjoyable collaborations on topics related to the contents of these lectures. I am grateful to Michał Przaszałowicz and the Organisers of the Zakopane school for the opportunity to speak, and especially to the students for making the lectures so much fun. I am supported by STFC and the European Research Council under the European Union's Seventh Framework Programme (FP7/2007–2013), ERC Grant agreement STG 279943, Strongly Coupled Systems.

#### REFERENCES

- [1] O. Aharony *et al.*, *Phys. Rep.* **323**, 183 (2000) [arXiv:hep-th/9905111].
- [2] S.A. Hartnoll, *Class. Quantum Grav.* **26**, 224002 (2009) [arXiv:0903.3246 [hep-th]].
- [3] J. McGreevy, *Adv. High Energy Phys.* **2010**, 723105 (2010) [arXiv:0909.0518 [hep-th]].
- [4] J.M. Maldacena, *Adv. Theor. Math. Phys.* **2**, 231 (1998) [arXiv:hep-th/9711200].
- [5] S.S. Gubser, I.R. Klebanov, A.M. Polyakov, *Phys. Lett.* **B428**, 105 (1998) [arXiv:hep-th/9802109].

- [6] E. Witten, *Adv. Theor. Math. Phys.* **2**, 253 (1998) [arXiv:hep-th/9802150].
- [7] E. D'Hoker, D.Z. Freedman, arXiv:hep-th/0201253.
- [8] Z.Q. Li *et al.*, *Nature Phys.* **4**, 532 (2008).
- [9] S. Sachdev, *Quantum Phase Transitions*, Cambridge University Press, 2011.
- [10] A.J. Leggett, *Quantum Liquids: Bose Condensation and Cooper Pairing in Condensed-matter Systems*, Oxford University Press, 2006.
- [11] D. van der Marel *et al.*, *Nature* **425**, 271 (2003) [arXiv:cond-mat/0309172].
- [12] T. Kato, M. Imada, *J. Phys. Soc. Jpn.* **67**, 2828 (1998) [arXiv:cond-mat/9711208 [cond-mat.stat-mech]].
- [13] P.W. Anderson, *Phys. Rev.* **B55**, 11785 (1997) [arXiv:cond-mat/9506140].
- [14] M.R. Norman, A.V. Chubukov, *Phys. Rev.* **B73**, 140501(R) (2006) [arXiv:cond-mat/0511584 [cond-mat.supr-con]].
- [15] E. Witten, *Adv. Theor. Math. Phys.* **2**, 505 (1998) [arXiv:hep-th/9803131].
- [16] C.P. Herzog, D.T. Son, *J. High Energy Phys.* **0303**, 046 (2003) [arXiv:hep-th/0212072].
- [17] A. Chamblin, R. Emparan, C.V. Johnson, R.C. Myers, *Phys. Rev.* **D60**, 064018 (1999) [arXiv:hep-th/9902170].
- [18] C.P. Herzog, P. Kovtun, S. Sachdev, D.T. Son, *Phys. Rev.* **D75**, 085020 (2007) [arXiv:hep-th/0701036].
- [19] G.T. Horowitz, J.E. Santos, D. Tong, *J. High Energy Phys.* **1211**, 102 (2012) [arXiv:1209.1098 [hep-th]].
- [20] G.T. Horowitz, J.E. Santos, D. Tong, *J. High Energy Phys.* **1207**, 168 (2012) [arXiv:1204.0519 [hep-th]].
- [21] S.A. Hartnoll, D.M. Hofman, *Phys. Rev. Lett.* **108**, 241601 (2012) [arXiv:1201.3917 [hep-th]].
- [22] A. Donos, S.A. Hartnoll, *Phys. Rev.* **D86**, 124046 (2012) [arXiv:1208.4102 [hep-th]].